

Coherent collisions of photorefractive solitons

Hongxing Meng and Greg Salamo

Department of Physics, University of Arkansas, Fayetteville, Arkansas 72701

Ming-feng Shih and Mordechai Segev

Department of Electrical Engineering, Princeton University, Princeton, New Jersey 08544

Received October 1, 1996

We present an experimental study of coherent collisions between one-dimensional bright photorefractive screening solitons in a bulk strontium barium niobate crystal. © 1997 Optical Society of America

Photorefractive spatial solitons¹⁻⁷ have become a subject of increased interest in the past few years. Several generic types of photorefractive self-trapping effects have been predicted and observed: quasi-steady-state,¹ photovoltaic,² and screening solitons,³⁻⁷ resonant self-trapping in photorefractive semiconductors,⁸ and of spatially incoherent beams.⁹

Collisions between solitons are perhaps the most fascinating features of self-trapped beams, since, in many respects, solitons interact like particles.¹⁰ Although a large body of literature on the theory of Kerr and non-Kerr soliton collisions exists (e.g., Refs. 10-12), very few experiments on collisions of spatial solitons have been reported. Such observations thus far include collisions of Kerr-type solitons in liquid CS₂ (Ref. 13) and in glass waveguides¹⁴ and of two-dimensional (2D) solitons in a saturable nonlinear medium.¹⁵

Recently, the first observation of collisions between mutually incoherent 2D photorefractive solitons was reported.¹⁶ Here we report observations of coherent collisions between photorefractive solitons. The solitons exert repulsion or attraction forces upon each other, depending on the initial relative phase. For in-phase collision, we find that the solitons fuse to a joint solution of the same or a broader width, which can be predicted from the soliton existence curve.

Collisions between photorefractive solitons possess several unique features. First, when two optical beams intersect in a photorefractive medium, their interference gives rise to refractive-index gratings that couple the beams to each other by energy exchange and phase coupling. The strength of a two-beam-coupling interaction depends on the period the interference grating and, for periods much larger than the Debye length (Λ_D), the resultant space-charge field can be approximated as $(k_B T/q) \nabla I / (I + I_b + I_d)$, where I , I_b , and I_d are the intensities of the interfering beams, a uniform background illumination, and the dark irradiance, respectively, k_B is Boltzman's constant, T is the temperature, and q is the electron charge. Second, the response time of photorefractive materials is inversely proportional to $I + I_b + I_d$. One can take advantage of the finite response time and observe collisions of solitons that are mutually incoherent, i.e., their relative phase (therefore their interference) varies randomly in time much faster than the medium can respond, hence the two-beam-coupling interaction is totally eliminated (now $\nabla I = \nabla I_1 + \nabla I_2$, leading to

self-bending¹⁶ of both solitons). Incoherent collisions between photorefractive solitons¹⁷ were found to be subject to the optical guiding properties of the waveguides induced by each of the solitons, which in turn are controlled by the soliton existence curve.¹⁸ Here we study coherent collisions between photorefractive solitons. Coherent collisions will be subject to (a) the waveguiding properties of the soliton-induced intersecting waveguides,¹⁹ which apply to all interacting solitons; (b) coherent attraction-repulsion forces, which apply to coherent soliton interactions only, and (c) two-beam-coupling processes, which apply to photorefractive spatial solitons only. For simplicity, we minimize (c) and study coherent collisions of photorefractive solitons with as little two-beam coupling as possible. Since for coherent collisions the interacting beams must be phase coherent to each other at all times, one cannot eliminate two-beam coupling by reducing the mutual coherence. Instead, we take advantage of the dependence of two-beam coupling on the grating period and study collisions of initially parallel-propagating solitons. The interference of two parallel-propagating beams gives rise to a grating of an infinite period, which minimizes ∇I and thus two-beam coupling. In practice, the solitons repel or attract each other, thereby introducing a small angle between them even if they are initially launched in parallel. Here this angle is always smaller than 1°, giving rise to a space-charge field smaller than 150 V/cm, which is much smaller than the field that supports the soliton (~ 2.5 kV/cm). Therefore two-beam coupling is reduced to self-bending of each beam¹⁶ with a minor effect on the collision. However, if we start with a nonzero initial angle between the beams, two-beam coupling is greatly enhanced. Here, we limit our study to collisions between initially parallel-propagating solitons.

The nonlinear change in the refractive index that gives rise to 1D bright photorefractive screening solitons³⁻⁵ is proportional to $(I_b + I_d)/(I + I_b + I_d)$, a form similar to that of solitons in saturable nonlinear media.¹² Screening solitons are characterized by an existence curve^{5,18} that relates the soliton width $\Delta \xi$ to $u_0^2 = I(0)/(I_b + I_d)$, the so-called intensity ratio. $\Delta \xi = \Delta x k n_b^2 (r_{\text{eff}} V/l)^{1/2}$ is a dimensionless soliton width that reaches a minimum at $u_0 = 1.6$, Δx is the actual soliton width (FWHM), $k = 2\pi/\lambda$, r_{eff} is the effective electro-optic coefficient, and V is the voltage

applied across the crystal of width l . While small deviations of the parameters from this curve are restrained by the soliton stability features, large deviations cannot support a soliton. The soliton existence curve is shown in Fig. 1 (solid curve) along with the (dashed) curve that shows what we measured in our experiments with a strontium niobate crystal of $n_b = 2.35$, $r_{\text{eff}} = r_{33} = 194 \text{ pm/V}$, $\lambda = 515 \text{ nm}$, and $l = 6 \text{ mm}$. The experimental curve is slightly offset from the theoretical curve to somewhat higher values of $\Delta\xi$ and u_0 for several reasons,¹⁸ the primary one being partial guidance of the background illumination by the soliton-induced waveguide (since $r_{13} \neq 0$).

Coherent collisions of screening solitons can be explained intuitively by the soliton existence curve and the interference between the evanescent tails of the interacting beams.¹⁰ When the initial relative phase is π the solitons destructively interfere in the region between them, thus effectively reducing the refractive index there. This is equivalent to a repulsive force between the solitons, and the solitons diverge from each other. This behavior is expected for any point on the existence curve. Attraction between screening solitons is far more intriguing, since the outcome depends on the location of the soliton parameters on the existence curve. Consider first the collision of two in-phase, initially parallel-propagating, identical solitons, each with u_0 slightly smaller than that of the existence curve minimum (point A, Fig. 1). Because the solitons constructively interfere in the region between them, they effectively increase the refractive index there, attract each other, and eventually merge. The combined beam has twice the intensity ratio, or $\sqrt{2}u_0$ (point B). However, points A and B possess the same $\Delta\xi$ value, meaning that, since all other parameters are unchanged, the combined beam has the same Δx width as each of the individual solitons. Thus, in the vicinity of the minimum in the existence curve, we expect two colliding in-phase solitons to fuse to a combined soliton of the same initial width. Next, consider two such colliding solitons, each with u_0 larger than that of the existence curve minimum (point C). Again, the solitons attract each other and merge to form a combined beam, but now the fused beam with twice the initial u_0^2 (or $\sqrt{2}u_0$) is at a point with a greater $\Delta\xi$ value on the curve (point D). The width of the fused soliton will therefore be equal to $(\Delta\xi \text{ at point D})/(\Delta\xi \text{ at point C})$ times the initial width. Thus, at u_0 values greater than the minimum in the existence curve, we expect two colliding in-phase solitons to fuse to a combined soliton wider than the initial width of each individual soliton. Finally, collisions of in-phase screening solitons in the $u_0^2 \ll 1$ region (point E) are expected to behave similarly to Kerr solitons, since at this limit screening solitons are almost identical to Kerr solitons.⁷ Thus, two such in-phase colliding solitons will undergo cycles of attraction–merging–splitting¹⁴ between points E and F. All cases of initial phase other than zero or π are expected to exhibit an intermediate behavior that breaks the symmetry between the interacting solitons.

In the experiment we launch two 1D soliton beams, a and b, using cylindrical lenses. The $10\text{-}\mu\text{m}$ FWHM wide beams are launched parallel to each other with

an $18\text{-}\mu\text{m}$ separation along the 6-mm -long crystalline a axis. The collision occurs in the plane defined by the narrow dimension of the solitons and the propagation axis. The beams are extraordinarily polarized, with their minimum waist at the input face of the crystal being nearly uniform (4 mm long) in the other transverse dimension. An ordinarily polarized beam uniformly illuminates the crystal to establish the background illumination $I_b \gg I_d$. We control the relative phase between the solitons with a tilted glass slide in one of the beams. We first launch solitons a and b separately. Since most of the voltage drop occurs in the regions outside the solitons, and since each soliton is much narrower than l , we can generate solitons a and b simultaneously, using the same voltage as for a single soliton (of the same width as a and b).¹⁷ We image the beams at the output face of the crystal onto a CCD camera with $\pm 1\text{-}\mu\text{m}$ resolution.

First, we launch two solitons, each with intensity ratio $u_0^2 = 8.5$, which correspond to point A in Fig. 1 (see Fig. 2a). With zero applied voltage, both beams diffract and are almost indistinguishable (Fig. 2b). With $V = 1250 \text{ V}$ across $l = 6 \text{ mm}$, two planar solitons form when launched separately (Fig. 2c; the solid and dashed profiles of Figs. 2a–2c correspond to separately launched beams). Then we observe the collision by launching the solitons simultaneously. When the relative input phase is zero, the solitons merge (fuse) and form an output beam of the same width as each of the input beams (Fig. 2d). This corresponds to the transition from point A to point B on Fig. 1. When the relative input phase is π , the solitons repel each other, increasing their separation at the output face of the crystal to $46 \mu\text{m}$, thus diverging from each other at 0.27° angle (Fig. 2f). In the intermediate case of $\pi/2$ (Fig. 2e), the output is two solitons separated by $35 \mu\text{m}$ (0.16° divergence angle) with unequal amplitudes.

Two solitons are then launched, each with intensity ratio $u_0^2 = 20$, which corresponds to point C on Fig. 1. Photographs and profiles of the separately launched input and diffracted output beams (at $V = 0$) are shown in Figs. 3a and 3b, respectively. With $V = 1700 \text{ V}$ applied, the separately launched beams form planar solitons (Fig. 3c). Notice that the solitons now require a higher voltage than in the $u_0^2 = 8.5$ case, in accordance with the existence curve^{5,18} (Fig. 1). Then, we observe the collision by launching the solitons

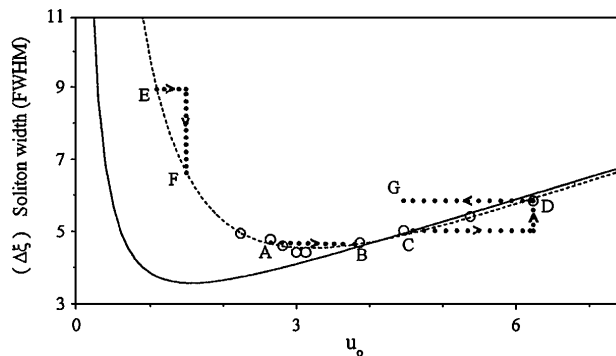


Fig. 1. Theoretical (solid) and experimental (dashed) plots of the normalized soliton width as a function of u_0 . Open circles correspond to experimentally measured solitons.

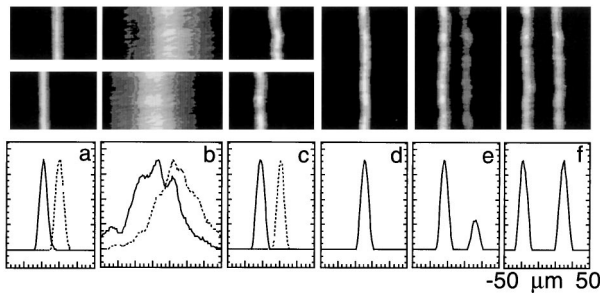


Fig. 2. Photographs and beam profiles at the input and exit faces of the crystal for intensity ratio 8.5: a, input beams; b, diffracted output beams at zero voltage; c, output soliton beams when launched separately, and d–f, output of the soliton collision for the 0, $\pi/2$, and π relative input phases, respectively.

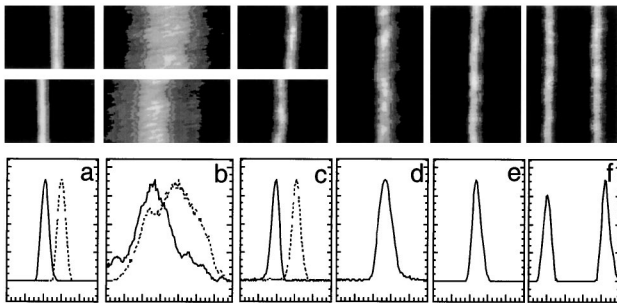


Fig. 3. Same as Fig. 2 but for intensity ratio 20: a, input beams; b, diffracted output beams at zero voltage; c, output soliton beams when launched separately; d, e, collision output for 0 relative input phase with $V = 1700$ and $V = 2400$ V, respectively; and f, collision output for π relative input phase.

simultaneously. For zero relative input phase, the solitons merge (fuse) and form a wider output beam (of $13 \mu\text{m}$ FWHM) than each of the input beams (Fig. 3d). This corresponds to the transition from point C to D on Fig. 1. Since, except for the width, all parameters are the same in both points, the ratio $(\Delta\xi \text{ at point D})/(\Delta\xi \text{ at point C})$ is equal to the (combined width Δx at point D)/(individual width Δx of each soliton at point C) = 1.3. Only when the voltage is increased to 2400 V does the fused beam narrow (Fig. 3e) to the width of each of the input beams. However, if we launch each beam separately with this increased voltage, each beam alone cannot form a soliton, since it corresponds to a large deviation from the existence curve (point G), which gives rise to instability and beam breakup.^{7,18} When the relative phase is adjusted to π , the solitons repel each other, increasing their output separation to $60 \mu\text{m}$, thus diverging at 0.4° angle (Fig. 3f). Note the increased repulsion between the solitons compared with that of the $u_0^2 = 8.5$ case (Fig. 2e), which is expected because the nonlinear-index change scales with $\Delta\xi^2 \propto V$ and is now larger. In the intermediate case of $\pi/2$, the colliding solitons follow the same trend as for $u_0^2 = 8.5$: emerging as two separate solitons with unequal amplitudes. Similar results were found for $u_0^2 = 39$.

Collisions of solitons with intensity ratios much smaller than the existence curve minimum are expected to resemble collisions of Kerr-type solitons.

However, as we try to generate 1D solitons with $u_0^2 \ll 1$ (point E, Fig. 1), the output beams suffer from severe longitudinal and transverse modulation instabilities.¹⁸ This is expected since, for $u_0^2 \ll 1$, screening solitons are almost identical to Kerr solitons,⁵ which suffer from strong transverse instabilities in a bulk medium. The instability is arrested at larger intensity ratios, where the photorefractive nonlinearity becomes saturated. In fact, no instability is observed in all our experiments as long as the parameters of the self-trapped beams are on the existence curve.

In conclusion, we have reported what is believed to be the first experimental observation of coherent collisions between photorefractive solitons.

This research was supported by the U.S. Army Research Office and the National Science Foundation.

References

1. M. Segev, B. Crosignani, A. Yariv, and B. Fischer, *Phys. Rev. Lett.* **68**, 923 (1992); G. Duree, J. L. Shultz, G. Salamo, M. Segev, A. Yariv, B. Crosignani, P. DiPorto, E. Sharp, and R. Neurgaonkar, *Phys. Rev. Lett.* **71**, 533 (1993).
2. G. C. Valley, M. Segev, B. Crosignani, A. Yariv, M. M. Fejer, and M. Bashaw, *Phys. Rev. A* **50**, R4457 (1994); M. Taya, M. Bashaw, M. M. Fejer, M. Segev, and G. C. Valley, *Phys. Rev. A* **52**, 3095 (1995).
3. M. Segev, G. C. Valley, B. Crosignani, P. DiPorto, and A. Yariv, *Phys. Rev. Lett.* **73**, 3211 (1994).
4. D. N. Christodoulides and M. I. Carvalho, *J. Opt. Soc. Am. B* **12**, 1628 (1995); *Opt. Commun.* **118**, 569 (1995).
5. M. Segev, M. Shih, and G. C. Valley, *J. Opt. Soc. Am. B* **13**, 706 (1996).
6. M. D. Iturbe-Castillo, P. A. Marquez-Aguilar, J. J. Sanchez-Mondragon, S. Stepanov, and V. Vysloukh, *Appl. Phys. Lett.* **64**, 408 (1994).
7. M. Shih, M. Segev, G. C. Valley, G. Salamo, B. Crosignani, and P. DiPorto, *Electron. Lett.* **31**, 826 (1995); *Opt. Lett.* **21**, 324 (1996).
8. M. Chauvet, S. A. Hawkins, G. Salamo, M. Segev, D. F. Bliss, and G. Bryant, *Opt. Lett.* **21**, 1333 (1996).
9. M. Mitchell, Z. Chen, M. Shih, and M. Segev, *Phys. Rev. Lett.* **77**, 490 (1996).
10. A. W. Snyder and A. P. Sheppard, *Opt. Lett.* **18**, 482 (1993); *Phys. Rev. Lett.* **77**, 271 (1996).
11. V. E. Zakharov and A. B. Shabat, *Sov. Phys. JETP* **34**, 62 (1972).
12. S. Gatz and J. Herrmann, *IEEE J. Quantum Electron.* **28**, 1732 (1992); *J. Opt. Soc. Am. B* **8**, 2296 (1991).
13. F. Reynaud and A. Barthelemy, *Europhys. Lett.* **12**, 401 (1990).
14. J. S. Aitchison, A. M. Weiner, Y. Silberberg, M. K. Oliver, J. L. Jackel, D. E. Leaird, E. M. Vogel, and P. W. Smith, *Opt. Lett.* **15**, 471 (1990); *J. Opt. Soc. Am. B* **8**, 1290 (1991).
15. V. Tikhonenko, J. Christou, and B. Luther-Davies, *Phys. Rev. Lett.* **76**, 2698 (1996); *J. Opt. Soc. Am. B* **12**, 2046 (1995).
16. Self-bending of photorefractive solitons was predicted in Ref. 4 and observed in Ref. 9.
17. M. Shih and M. Segev, *Opt. Lett.* **21**, 1538 (1996).
18. K. Kos, H. Meng, G. Salamo, M. Shih, and M. Segev, *Phys. Rev. E* **53**, R4330 (1996).
19. M. Shih, M. Segev, and G. Salamo, *Opt. Lett.* **21**, 931 (1996).